

# Molecular dynamics study of diffusion of formaldehyde in ice

V. Ballenegger<sup>a,\*</sup>, S. Picaud<sup>a</sup>, C. Toubin<sup>b</sup>

<sup>a</sup> *Laboratoire de Physique Moléculaire, UMR CNRS 6624, Faculté des Sciences, La Bouloie, Université de Franche-Comté, 25030 Besançon Cedex, France*

<sup>b</sup> *Laboratoire de Physique des Lasers Atomes et Molécules, UMR CNRS 8523, Centre d'Etudes et de Recherches Lasers et Applications, Université des Sciences et Technologies de Lille, Bat. P5, 59655 Villeneuve d'Ascq Cedex, France*

Received 23 August 2006; in final form 2 October 2006

Available online 13 October 2006

## Abstract

We report a Molecular Dynamics simulation study of the diffusion process of formaldehyde (CH<sub>2</sub>O) in proton-disordered ice Ih at atmospheric pressure, in the temperature range 200–273 K. CH<sub>2</sub>O molecules diffuse in ice predominantly by jumping between B sites (bond-breaking mechanism), but substitutional diffusion can also be observed. At 260 K, the diffusion constant is predicted to be  $4 \times 10^{-7}$  cm<sup>2</sup>/s with the TIP4P–Ew water model, and  $3 \times 10^{-7}$  cm<sup>2</sup>/s with the TIP4P/Ice water model.

© 2006 Elsevier B.V. All rights reserved.

## 1. Introduction

Interest in the interactions between trace gases and ice surfaces has been stimulated in recent years by the recognition of the crucial role that ice surfaces can play in catalytic ozone destruction and in partitioning of photochemically active trace gases between air and ice [1]. More recently, the role of the snowpack in the atmospheric chemistry of gases such as formaldehyde (CH<sub>2</sub>O) and NO<sub>x</sub> above snow-covered surfaces has also been evidenced and it appears now essential to take into account the trace gases/snow interactions in the atmospheric studies above polar regions [2–4].

However, understanding the possible exchange of such trace gases between snow and the lower atmosphere requires the knowledge of their incorporation, diffusion, and release mechanisms in snow crystals. Recent studies have in particular focused on the formaldehyde molecule [5–11], because its photolysis produces oxidizing radicals that enhance the oxidizing capacity of the atmosphere in polar regions, where the other sources of these radicals are reduced. Although the location of CH<sub>2</sub>O in snow

appeared controversial from the conclusions of these studies, the diffusion coefficient of CH<sub>2</sub>O in ice is certainly one among several key parameters that need to be known to quantify the contribution of the snowpack to the atmospheric chemistry of CH<sub>2</sub>O [11].

Unfortunately, diffusion measurements of trace gases in ice are scarce due to experimental challenges. Conflicting results have been reported for HCl, with diffusion coefficients ranging from  $D \approx 10^{-5}$  cm<sup>2</sup>/s to  $D \approx 10^{-13}$  cm<sup>2</sup>/s at  $T = 185$  K [12–17]. This wide range of diffusion coefficients has been attributed to different ice preparation conditions, species concentrations, variable defects and grain boundaries, and trapping phenomena [17]. Notice that a strong acid such as HCl certainly dissociates at the above temperatures, influencing thereby the diffusion mechanism. A partially oxidized organic compound such as formaldehyde does not dissociate in ice, but the experimental studies of its diffusion are still very rare. To our knowledge, only one value can be found in the literature, namely  $D \approx 8 \times 10^{-11}$  cm<sup>2</sup>/s at 258 K [11]. A similar value has been reported for the diffusion of methanol in ice, but at a much lower temperature ( $D \approx 2 \times 10^{-11}$  cm<sup>2</sup>/s at 185 K) [18].

In the present Letter, we use Molecular Dynamics (MD) simulations to characterize the diffusion mechanisms of formaldehyde in ice at a molecular level, and to provide an accurate value of the diffusion coefficient

\* Corresponding author. Fax: +33 3 81 66 64 75.

E-mail address: [vincent.ballenegger@univ-fcomte.fr](mailto:vincent.ballenegger@univ-fcomte.fr) (V. Ballenegger).

of CH<sub>2</sub>O in a perfect 3D proton-disordered ice Ih crystal at atmospheric pressure, for temperatures in the range 200–273 K. Indeed, such simulations have been recently proved to be an accurate tool for investigating the diffusion mechanisms of small guest particles in ice, such as He, H<sub>2</sub>O, CO<sub>2</sub>, N<sub>2</sub>, O<sub>2</sub> and CH<sub>4</sub> [19–22].

## 2. Computational method

### 2.1. Intermolecular potentials

Many effective pair potentials have been devised to simulate water at liquid densities. We decided to use the TIP4P model of Jorgensen et al. [23], as reparametrized by Horn et al. [24] for use with Ewald summations, because this four-site model is a good compromise between accuracy and speed of computation. The melting temperature of TIP4P–Ew ice at atmospheric pressure is  $244 \pm 3$  K [25]. Although higher than the melting temperatures of the SPC/E and standard TIP4P models, this value is still significantly below the experimental result 273 K. For comparison purposes, we performed also the same simulations with the new TIP4P/Ice model [26], which was designed to reproduce correctly the melting temperature of ice Ih.

For consistency with the chosen water model, we treat the formaldehyde molecule as a rigid body having only translational and rotational degrees of freedom. The interaction sites of a CH<sub>2</sub>O molecule are taken from the OPLS force field, and are summarized in Table 1 of Ref. [27]. The cross interaction between a formaldehyde and a water molecule is defined by using the usual Lorentz–Berthelot combining rules (geometric mean of  $C^{(6)}$  and  $C^{(12)}$  van der Waals coefficients) for each site–site interaction pair. The combination of OPLS and TIP4P parameters has been validated in Ref. [27].

As the models used in this study are slightly different from the original TIP4P model, we carried out energy min-

imization calculations for the CH<sub>2</sub>O–H<sub>2</sub>O dimer, and compared with quantum chemistry calculations (B3LYP/6-31+G(d,p) and MP2/6-311+G(d,p)). Both models, TIP4P–Ew and TIP4P/Ice, lead to the same geometry with comparable bond lengths and bond angles. However this configuration is slightly distorted when compared to the ab initio or TIP4P dimer configurations. From an energetic point of view, very similar binding energies are obtained with TIP4P–Ew (–229 meV) compared to TIP4P (–221 meV) and ab initio values (–220 meV (B3LYP) and –228 meV (MP2)), whereas the TIP4P/Ice model tends to overestimate the CH<sub>2</sub>O–H<sub>2</sub>O interaction (–245 meV). Since the energy discrepancies (more important in the case of the TIP4P/Ice) do not alter significantly the binding properties of CH<sub>2</sub>O with H<sub>2</sub>O, both models should reproduce the CH<sub>2</sub>O–H<sub>2</sub>O and CH<sub>2</sub>O/ice interaction within reasonable accuracy.

### 2.2. Simulation details of ice Ih

The system consists in an orthorhombic simulation cell, with edges  $a \approx 2.69$ ,  $b \approx 3.14$  and  $c \approx 2.89$  (in nm units), containing 768 water molecules for one CH<sub>2</sub>O molecule. In the starting configuration, the water molecules are arranged according to the crystallographic structure of hexagonal ice Ih [28]. The protons are oriented randomly, under the restriction that the Bernal–Fowler ice rules are respected [28] and that the system carries no net dipole moment. The simulation cell accommodates a lattice made up of 8 layers, each containing  $6 \times 8$  hexagonal rings, that are stacked vertically (i.e. along the  $z$ - or  $c$ -axis). The formaldehyde molecule is placed initially at the centre of an interstitial cavity.

The MD simulations were performed using GROMACS [29], in the NpT ensemble. The temperature and pressure are kept constant by coupling the system to a Berendsen thermostat and barostat. Periodic boundary conditions are applied in all three directions, and long-range electrostatic interactions are calculated using Ewald summations (Ewald splitting parameter  $\alpha = 3.47 \text{ nm}^{-1}$ ). The cut-off for Lennard-Jones and real-space coulombic interactions was set to 0.9 nm. The Smooth Particle Mesh Ewald method was used to compute reciprocal electrostatic forces and energies; the mesh had a size of  $5 \times 6 \times 6$  cells, and cubic splines were used.

The equations of motion were integrated using the leap-frog algorithm with a time step of 2 fs. Each production run lasted at least 100 ns. This very long simulation time is necessary to gather enough statistics on the diffusion of the CH<sub>2</sub>O molecule, which is a slow process at low temperatures.

### 2.3. Determination of diffusion constant

In an isotropic medium, the diffusion constant  $D$  of a molecule is related to its mean square displacement (MSD) according to Einstein's formula

Table 1  
Diffusion constant of formaldehyde in ice, computed with the TIP4P–Ew water model (a) and with the TIP4P/Ice water model (b)

$T$ (K)	$D$ ( $10^{-7} \text{ cm}^2/\text{s}$ )
<i>(a) TIP4P–Ew</i>	
210	0.44
220	0.78
230	1.45
235	1.80
240	1.92
245	2.27
250	2.37
<i>(b) TIP4P/Ice</i>	
230	1.00
240	1.53
250	2.73
260	2.31
270	3.29
275	3.71

$$D = \lim_{t \rightarrow \infty} \frac{\langle (\mathbf{r}(t) - \mathbf{r}(0))^2 \rangle}{6t} \quad (1)$$

( $\mathbf{r}(t)$  is the position of the centre of mass of the molecule). Admittedly, ice is anisotropic, but we observed in our simulations that the diffusion of formaldehyde parallel and perpendicular to the  $c$ -axis are of the same order of magnitude. We analyse therefore the simulation data by using the isotropic formula.

The ensemble average in the MSD cannot be performed here as usual by averaging over different molecules (since there is only one formaldehyde molecule in the system). The MSD must therefore be computed by averaging the squared displacement measured in several independent trajectories. (This averaging is important because the molecule can travel back and forth and end up very close to its starting position at the end of a simulation). In practice, we use a very long trajectory (duration  $T_{\text{sim}} \approx 100$  ns) that we regard as being composed of  $N$  ‘independent’ trajectories of duration  $\Delta t = T_{\text{sim}}/N$ . The ensemble average is then approximated by

$$\langle (\mathbf{r}(t) - \mathbf{r}(0))^2 \rangle \simeq \frac{\sum_{i=0}^{N-1} \Theta(T_{\text{sim}} - t - t_i) (\mathbf{r}(t + t_i) - \mathbf{r}(t_i))^2}{\sum_{i=0}^{N-1} \Theta(T_{\text{sim}} - t - t_i)} \quad (2)$$

where  $t_i = i\Delta t$  is the starting time of the  $i$ th segment of the trajectory, and  $\Theta$  is the Heaviside function. At short times,  $0 \leq t \leq \Delta t$ , the MSD is thus obtained as an average of the displacements observed in the  $N$  segments, while obviously less statistics is available at longer times. Fig. 1 contains an example of the above ‘ensemble’ averaging for the MSD of a typical trajectory. We use very small ‘restart’ times  $\Delta t = T_{\text{sim}}/N$  to ensure optimal exploitation of the data ( $\Delta t = 200$  ps is small enough for  $T_{\text{sim}} = 100$  ns).

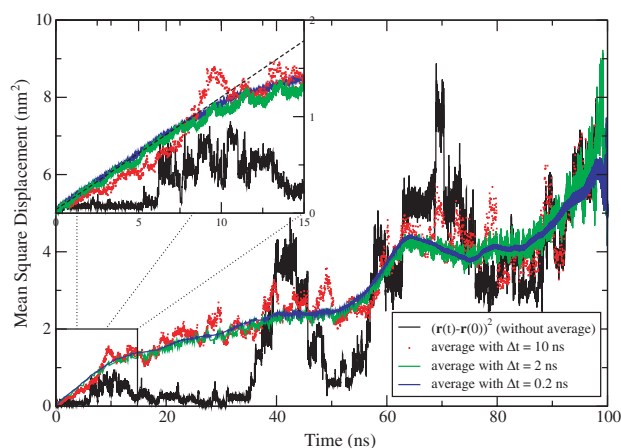


Fig. 1. Mean square displacement of a formaldehyde molecule in proton-disordered ice at 235 K. The ensemble average (2) is computed for three increasingly small ‘restart’ times  $\Delta t$ . The diffusion coefficient is obtained from the slope of a linear fit of the data for times  $t \leq 7$  ns, as shown in the inset (dashed line). Linear behaviour is not observed at larger times because of insufficient statistics.

### 3. Results and discussion

#### 3.1. Diffusion constant

The diffusion of formaldehyde in ice was simulated at constant atmospheric pressure for various temperatures in the range 210–275 K using two different water models: TIP4P–Ew and TIP4P/Ice (see previous section for simulation parameters). The diffusion constant is measured in each run using formulae (1) and (2), and Table 1 summarizes the results.

The highest temperatures chosen (250 K for TIP4P–Ew and 275 K for TIP4P/Ice) are slightly above the melting temperature of these models, but the ice crystal did not melt on the timescale of the simulation (100 ns). Such metastable superheated phases do not exist experimentally, but are known to occur in simulations of bulk systems [25,30], because simulation times are much shorter than the typical time needed to cross the activation energy barrier for melting.

Fig. 2 represents the evolution of the diffusion constant as a function of the (inverse) temperature for the two simulated models. The error bars are rough estimates of the uncertainties based on the convergence of  $D$ : they correspond to the maximum difference between  $D$  and the values of the diffusion constants which would be obtained by considering only the first, resp. the last, 50 ns of the simulation. For both models, the points clearly follow a linear relationship, showing that the diffusion process obeys, not surprisingly, to Arrhenius law

$$D = D_0 \exp(-E_{\text{diff}}/kT) \quad (3)$$

where  $E_{\text{diff}}$  is the activation energy of the diffusion process.

For the TIP4P–Ew model, we get  $E_{\text{diff}} \approx 20.2$  kJ/mol and  $D_0 \approx 5 \times 10^{-3}$  cm<sup>2</sup>/s, while  $E_{\text{diff}} \approx 14.3$  kJ/mol and  $D_0 \approx 2 \times 10^{-4}$  cm<sup>2</sup>/s for the TIP4P/Ice model. In the range 230–250 K, the diffusion constant predicted by both models agree within simulation uncertainties. With the results of the TIP4P/Ice model at higher temperatures

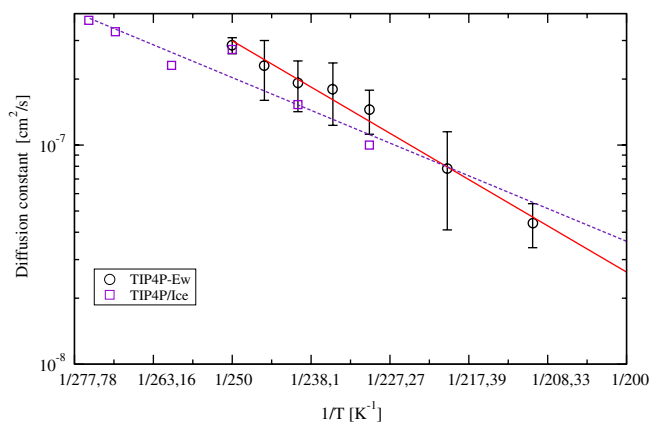


Fig. 2. Arrhenius plot of the diffusion constant of formaldehyde in ice Ih for two different water models.

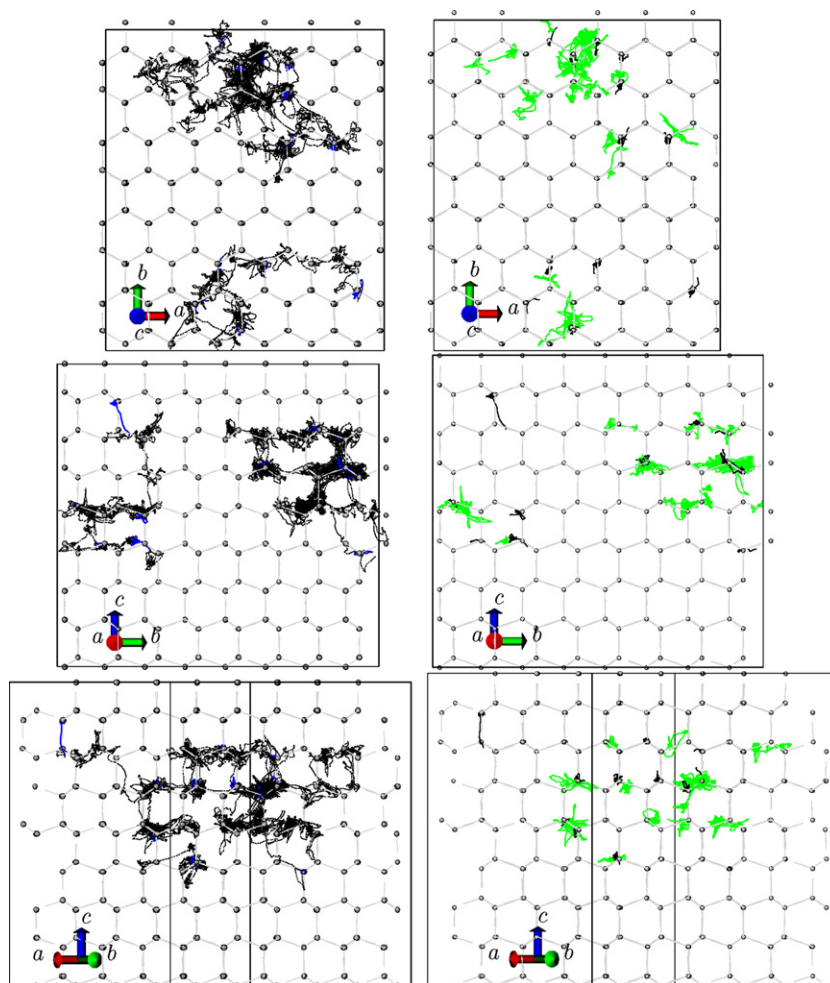


Fig. 3. Left column: Trajectory of the formaldehyde molecule (oxygen atom) during the first 70 ns of the simulation at 250 K (TIP4P–Ew water). The path is shown as a dotted line projected onto the (0001),  $(2\bar{1}\bar{1}0)$  and  $(1\bar{2}10)$  planes. Right column: some stable sites in the trajectory. The position of the oxygen atom is shown as a black line when the potential energy the formaldehyde molecule is at its low value. Gray lines represent the centre of mass of the molecule in stable sites with high potential energy.

(where statistics is quite good), we see however that the activation energy of the latter model is about 30% lower. The difference between the two models can be made smaller if we rescale the TIP4P results to interpret the value at the melting point of the model (245 K), as corresponding effectively to the experimental melting temperature (273 K), while leaving unchanged the result at the lowest simulated temperature (210 K). If predicting an accurate value of the activation energy is not easy, the simulations give however theoretical estimates for the order of magnitude of the diffusion constant in the whole temperature range 200–273 K.

### 3.2. Stable sites and diffusion mechanism

Fig. 3 shows the diffusion path followed by the formaldehyde molecule, or more precisely its oxygen atom, in the simulation at 250 K (in this section, all references are to the simulations performed with the TIP4P–Ew model). The trajectory of the O atom is projected onto the (0001),

$(2\bar{1}\bar{1}0)$  and  $(1\bar{2}10)$  planes<sup>1</sup>, and has been smoothed, by a running average over a 20 ps window, to reduce thermal noise. It has been shown by previous authors that a small apolar guest molecule, such as He, Ne, Ar or H<sub>2</sub>, diffuse by jumping between Tu (trigonal uncapped) interstitial sites, without distorting the ice lattice [19,21]. The Tu site is located on the axis of the open hexagonal channels along the *c*-axis, and can accommodate larger molecules than the Tc interstitial site (see Fig. 4). It has been shown moreover that large apolar molecules, such as O<sub>2</sub>, N<sub>2</sub> and CH<sub>4</sub>, diffuse in ice by jumping between so-called B (bond) sites, by the bond-breaking mechanism [19,22]. The *B* site is located at the centre of an O–O bond in the basal plane (the centre of an O–O bond parallel to the *c*-axis corresponds to a similar, but not crystallographically equivalent, Bc site). In the bond-breaking mechanism, the dominant

<sup>1</sup> In the Miller–Bravais notation appropriate for hexagonal structures, the third index is redundant [ $i = -h - k$  in  $(hki)$ ] and is used to show the equivalent directions by cyclic permutations of the indices.

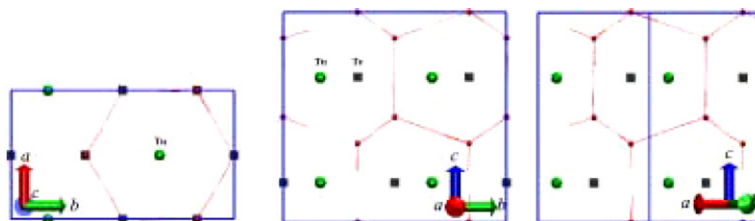


Fig. 4. Orthorhombic unit cell for ice Ih ( $a = 4.519 \text{ \AA}$ ,  $b = a\sqrt{3}$ ,  $c = 7.357 \text{ \AA}$  at 253 K). The locations of the Tu and Tc interstitial sites are shown by little spheres and cubes respectively. The Tu sites are located on the axis of the open hexagonal channels along the  $c$ -axis, midway between two layers. The smaller Tc (trigonal capped) interstitial sites are located at the same height, midway between oxygen atoms that are aligned vertically (i.e. along the  $c$ -axis) and that are not adjacent in a hexagonal ring.

factor governing the diffusion is the repulsive steric interactions between the guest and the  $\text{H}_2\text{O}$  molecules. These interactions distort the structure of the ice lattice, breaking an O–O bond to accommodate the guest molecule in a B site. The two water molecules of the former O–O bond are displaced from their original lattice positions, and are pushed towards them because of the remaining hydrogen bonds with the surrounding  $\text{H}_2\text{O}$  molecules.

A comparison of the diffusion path of  $\text{CH}_2\text{O}$  (Fig. 3) and the positions of the interstitial sites (Fig. 4) shows that this molecule does not diffuse via interstitial sites: the Tu and Tc sites do not accommodate the large  $\text{CH}_2\text{O}$  molecule. This finding is consistent with the results obtained for  $\text{N}_2$ ,  $\text{O}_2$ ,  $\text{CH}_4$  and  $\text{CO}_2$  [19,22].

Identifying the stable sites of  $\text{CH}_2\text{O}$  in the ice lattice is a difficult task. It is done both by analysing the time evolution of the potential energy  $E_f(t)$  of the formaldehyde molecule, and by monitoring the positions  $\mathbf{r}_i(t)$  of different sites ( $i = \text{centre of mass, oxygen, carbon}$ ) of the molecule along the trajectory.  $E_f(t)$  is plotted in Fig. 5 for the diffusion path represented in Fig. 3 (a running average has been applied to reduce thermal noise). This quantity takes either a low value of about  $-52 \text{ kJ/mol}$ , or a higher value of about  $-37 \text{ kJ/mol}$ . The lower value corresponds to configurations with in average two hydrogen bonds between the oxy-

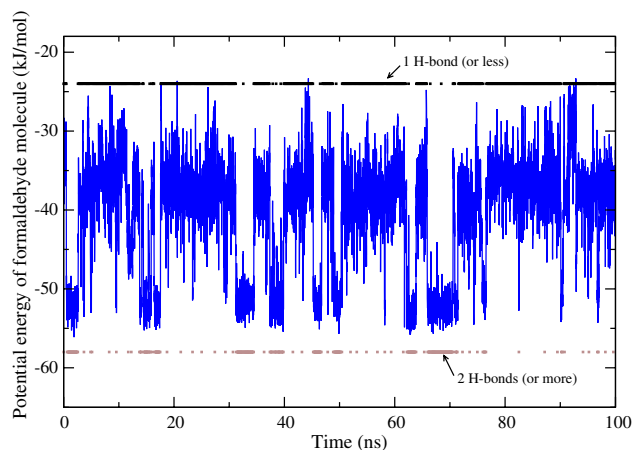


Fig. 5. Potential energy of a diffusing formaldehyde molecule at 250 K. The discontinuous black and grey horizontal lines indicate the time during which the formaldehyde forms one, resp. more than one, hydrogen bond (in average) with the surrounding water molecules.

gen atom and the neighbouring water molecules. Although these configurations minimize  $E_f(t)$ , they occur only 24% of the time at the considered temperature (250 K). The higher energy sites are favoured because they lead to a lower total energy for the system ( $\text{CH}_2\text{O}$  and lattice). The analysis of configurations  $\mathbf{r}_f(t)$  characterized by the lower values of  $E_f$  shows that they correspond to  $\mathbf{r}_\text{O}$  positions at a lattice point normally occupied by the oxygen atom of a water molecule (see Fig. 3). These sites correspond therefore to the formaldehyde replacing a water molecule, which has been pushed out from its lattice position. As a consequence, jumps between such sites correspond to the so-called ‘substitutional’ diffusion mechanism. Configurations with high energies  $E_f$  correspond by contrast to the formaldehyde occupying a B site, as shown by the position  $\mathbf{r}_\text{CM}(t)$  of its centre of mass (see Fig. 3). Formaldehyde diffuses therefore predominantly by jumping between B sites by the bond-breaking mechanism, though substitutional diffusion does also occur.

#### 4. Conclusion

In this study, long simulations (100 ns) were used to elucidate the diffusion mechanism of formaldehyde in ice Ih, and to get accurate values for the diffusion constant of this compound. In the considered temperature range 200–273 K, we found that  $\text{CH}_2\text{O}$  diffuses predominantly by jumping between B sites, though substitutional diffusion does also happen. Because formaldehyde can accept two hydrogen bonds with surrounding water molecules, its diffusion path is more subtle than the pure bond-breaking mechanism that characterizes the diffusion of large apolar molecules.

The time over which the formaldehyde molecule jumps between stable sites is about 20 ps. Since this is one order of magnitude larger than the characteristic time of molecular motion (1 ps), free energy calculations can be used to calculate precisely the jump probability between B sites (using Transition State Theory [31]). The simulation times used in this study are however long enough to allow relatively accurate estimates of the diffusion constant. This quantity obeys Arrhenius law, as expected for an activated process. Using the activation energies reported after Eq. (3), we find that the diffusion constant of  $\text{CH}_2\text{O}$  at 260 K is  $D \approx 4 \times 10^{-7} \text{ cm}^2/\text{s}$  with the TIP4P–Ew water model,

and  $D \approx 3 \times 10^{-7} \text{ cm}^2/\text{s}$  with the TIP4P/Ice water model. These values are much larger than the experimental result of Perrier et al. [11], who measured  $D \approx 8 \times 10^{-11} \text{ cm}^2/\text{s}$  at 258 K in a macroscopic ice sample. Theory and experiment are known to agree in experimentally well controlled materials, such as in semiconductors and zeolites [32,33]. The present discrepancy may be due to trapping phenomena in the ice crystal, which inevitably contains defects and grain boundaries. Further experimental work on diffusion of  $\text{CH}_2\text{O}$  (and air molecules  $\text{O}_2$ ,  $\text{N}_2$ ,  $\text{CO}_2$ ,  $\text{CH}_4$ ) would be most welcome, especially if it probes the diffusion on a molecular scale in a single crystal.

### Acknowledgements

The various snapshots of the simulation cell have been produced with the program VMD (Visual Molecular Dynamics) [34]. The authors gratefully acknowledge the Programme National de Chimie Atmosphérique for financial support.

### References

- [1] J.H. Seinfeld, S.N. Pandis, *Atmospheric Chemistry and Physics*, Wiley, New York, 1998.
- [2] A.L. Sumner, P.B. Shepson, *Nature* 398 (1999) 230.
- [3] R.E. Honrath, M.C. Peterson, S. Guo, J.E. Dibbs, P.B. Shepson, B. Campbell, *Geophys. Res. Lett.* 26 (1999) 695.
- [4] A.E. Jones, R. Weller, P.S. Anderson, H.W. Jacobi, E.W. Wolff, O. Schrems, H. Miller, *Geophys. Res. Lett.* 28 (2001) 1499.
- [5] M.A. Hutterli, R. Rothlisberger, R.C. Bales, *Geophys. Res. Lett.* 26 (1999) 1691.
- [6] M.A. Hutterli, R.C. Bales, J.R. McConnell, R.W. Stewart, *Geophys. Res. Lett.* 29 (2002) 1029.
- [7] H.W. Jacobi et al., *Atmos. Environ.* 36 (2002) 2619.
- [8] A.K. Winkler, N.S. Holmes, J.N. Crowley, *Phys. Chem. Chem. Phys.* 4 (2002) 5270.
- [9] S. Perrier, S. Houdier, F. Dominé, A. Cabanes, L. Legagneux, A.L. Sumner, P.B. Shepson, *Atmos. Environ.* 36 (2002) 2695.
- [10] J.F. Burkhart, M.A. Hutterli, R.C. Bales, *Atmos. Environ.* 36 (2002) 2157.
- [11] S. Perrier, P. Sassin, F. Dominé, *Can. J. Phys.* 81 (2003) 319.
- [12] M.J. Molina, T.L. Tso, L.T. Molina, F.C. Wang, *Science* 238 (1987) 1253.
- [13] E.W. Wolff, R. Mulvaney, K. Oates, *Geophys. Res. Lett.* 16 (1989) 487.
- [14] F. Dominé, E. Thibert, E. Silvente, M. Legrand, J.L. Jaffrezo, *J. Atmos. Chem.* 21 (1995) 165.
- [15] E. Thibert, F. Dominé, *J. Phys. Chem. B* 101 (1997) 3554.
- [16] A.B. Horn, J. Sully, *J. Chem. Soc., Faraday Trans.* 93 (1997) 2741.
- [17] F.E. Livingston, S.M. George, *J. Phys. Chem. A* 105 (2001) 5155.
- [18] F.E. Livingston, J.A. Smith, S.M. George, *J. Phys. Chem. A* 106 (2002) 6309.
- [19] T. Ikeda-Fukazawa, S. Horikawa, T. Hondoh, K. Kawamura, *J. Chem. Phys.* 117 (2002) 3886.
- [20] A. Demurov, R. Radhakrishnan, B.L. Trout, *J. Chem. Phys.* 116 (2002) 702.
- [21] T. Ikeda-Fukazawa, K. Kawamura, T. Hondoh, *Chem. Phys. Lett.* 385 (2004) 467.
- [22] T. Ikeda-Fukazawa, K. Kawamura, T. Hondoh, *Mol. Sim.* 30 (2004) 973.
- [23] W.L. Jorgensen, J. Chandrasekhar, J.D. Madura, R.W. Impey, M.L. Klein, *J. Chem. Phys.* 79 (2005) 926.
- [24] H.W. Horn, W.C. Swope, J.W. Pitera, J.D. Madura, T.J. Dick, G.L. Hura, T. Head-Gordon, *J. Chem. Phys.* 120 (2004) 9665.
- [25] R. García Fernández, J.L.F. Abascal, C. Vega, *J. Chem. Phys.* 124 (2006), art. no 144506.
- [26] J.L.F. Abascal, E. Sanz, R. García Fernández, C. Vega, *J. Chem. Phys.* 122 (2005), art. no 234511.
- [27] B. Collignon, S. Picaud, *Chem. Phys. Lett.* 393 (2004) 457.
- [28] V.F. Petrenko, R.W. Whitworth, *Physics of Ice*, Oxford University Press, 1999.
- [29] E. Lindahl, B. Hess, D. van der Spoel, *J. Mol. Mod.* 7 (2001) 306–317. <http://www.gromacs.org>.
- [30] S.C. Gay, E.J. Smith, A.D.J. Haymet, *J. Chem. Phys.* 116 (2002) 8876.
- [31] B.H. Mahan, *J. Chem. Educ.* 51 (1974) 709.
- [32] V. Gusakov, *J. Phys.: Condens. Matter* 17 (2005) S2285.
- [33] M. Kawano, B. Vessal, C.R.A. Catlow, *J. Chem. Soc., Chem. Commun.* (1992) 879.
- [34] W. Humphrey, A. Dalke, K. Schulten, *J. Mol. Graphics* 14 (1996) 33.